Macromolecules

ARTICLE

pubs.acs.org/Macromolecules

Distinct Elastic Response to Hierarchical Nanostructures

Xiaomeng Zhu, Liquan Wang, and Jiaping Lin*

Shanghai Key Laboratory of Advanced Polymeric Materials, Key Laboratory for Ultrafine Materials of Ministry of Education, State Key Laboratory of Bioreactor Engineering, School of Materials Science and Engineering, East China University of Science and Technology, Shanghai 200237, China

ABSTRACT: We employed self-consistent field theory to elucidate the mechanical properties of $A(BC)_n$ multiblock copolymer in hierarchical lamellae-in-lamellar structures. Extension and shear moduli as well as Young's modulus have been characterized. A remarkable improvement of elastic modulus in the process of morphology transformation from lamella to lamellae-in-lamella was discovered. The mechanical response of hierarchical lamella is also shown to be dependent on the number of small-length-scale structures. From the physical origin of the enhanced mechanical properties, it was found that internal energy and conformational entropy of BC blocks play a predominate role in improving the elastic moduli in the hierarchical lamellar structures. Our findings are in agreement with the recent experimental observations and also yield guidelines for designing hierarchical materials with improved properties.

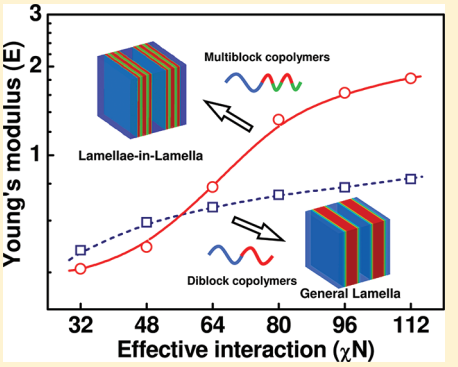

INTRODUCTION

Hierarchical structures can be observed in nature such as bone, shell, and attachment pads of geckos.[1−3] Such materials exhibit a structural hierarchy over many length scales. For example, sea shells comprise two to three levels of lamellar structure, and vertebral bone has seven levels of hierarchical structure.[4,5] In these hierarchical structures, each constituent at different nanometer scales exhibits its characteristic features, which leads to the complexity and variations of the enhanced composite macroscopic properties. For example, it has been demonstrated that intermediate filaments in cell are highly sensitive to applied forces and can sustain extremely large deformation of up to 300%, owing to their multiscale levels ranging from H-bonds to the cellular level.[6] For this reason, mimicking the nature to design and fabricate materials with hierarchical structures is of great interest from both theoretical and engineering viewpoints.

Up to now, various strategies have been developed for creating hierarchical nanostructures.[7−14] As ten Brinke et al. reported, supramolecular comb−coil block copolymers with low molecular weight compound linked to the block copolymer chains are capable of self-organizing into structure-in-structure morphologies.[15−18] These hierarchical structures possess double periodicities, including the large period of diblock copolymers and the small period of comb-shaped blocks. In addition, Matsushita et al. synthesized a series of linear multiblock copolymers such as $V(IS)_nIV$ and $V(IS)_nI$, where V, I, and S refer to poly(2-vinylpyridine), polyisoprene, and polystyrene, respectively.[19−22] Such copolymers can also self-assemble into various structure-in-structures, e.g., onionlike sphere and coaxial cylinder, with two different length scales. As these hierarchical structures were discovered, the morphology window of nanostructures self-assembled from copolymers was expanded, which lays a solid foundation for further studies on subjects such as mechanical properties.

Some primary investigations on hierarchical nanostructures revealed that the polymeric materials with multiple length scales can possess unique mechanical properties. For example, Bates et al. recently synthesized a new type of linear multiblock copolymers which are able to microphase-separate into hierarchical nanostructures.[23] These copolymer samples were observed to have the distinct mechanical properties.[24] The elastic property of such multiblock copolymers exhibits improved features in comparison with the block copolymers with simple architectures like AB and ABA types.[25−31] However, such structure−properties relationships of materials involving multiple periodicities are rarely acknowledged and little understood. Herein, we concerned the roles of hierarchical nanostructures in determining the elastic properties of materials.

Apart from the experiments, theoretical approaches,[32−37] such as self-consistent field theory (SCFT),[38−40] are useful tools to get an insight into the mechanical properties of polymeric materials. Tyler and Morse have used SCFT in reciprocal space to examine the linear elasticity of the body-centered cubic and gyroid phases of block copolymer.[41] It was found that the reduced elastic moduli are universal functions of interaction parameters, volume fraction, and block asymmetry. The SCFT was also employed to investigate the elastic properties of various systems, such as multiblock copolymers,[42] nanocomposites,[43] polydispersed diblock copolymers,[44] and ABC triblock copolymers.[45] Moreover, Maniadis et al. incorporated the elastic stress and strain fields into the SCFT and found that the local stress is reduced at interface but slightly enhanced in the vicinity of the interface.[46] In our group, the SCFT was applied for studying the

Received: June 21, 2011
Revised: September 4, 2011
Published: September 21, 2011

elastic properties of graft copolymers in lamellar phase.[47] The calculations revealed that the moduli can be tailored by the architectural parameters of graft copolymers. The SCFT results were found to be comparable to the existing experimental results. The success of the SCFT simulations makes it ready to be extended to predict the mechanical properties of materials with hierarchical structures.

In previous works, we predicted that various copolymer systems (e.g., $A(BC)_n$ multiblock copolymer) can self-assemble into hierarchically ordered nanostructures, such as lamellae-in-lamella, cylinders-in-lamellae, cylinders-in-cylinder, and spheres-in-sphere.[48−50] Herein, we adopted the real-space SCFT to investigate the elastic properties of $A(BC)_n$ multiblock copolymers in hierarchical lamellar structures. The extension and shear moduli were calculated for the $A(BC)_n$ copolymers in lamellae-in-lamellar phase. In addition, the physical origins of the hierarchical structure effects on the elastic properties were examined. It was discovered that the elastic moduli of the $A(BC)_n$ multiblock copolymers are enhanced significantly when the hierarchical nanostructures are formed. The moduli can be manipulated by changing the substructures at small-length scale and the internal energy contribution from BC blocks plays an important role in determining the moduli. We expect that the present work could provide useful information for designing advanced materials with hierarchical structures.

METHODS

We first introduce the linear elasticity model for multiblock copolymers in the lamellar phase. The details of the model have been described in the work by Thompson et al.[42] Here, we introduce the methodology briefly. In the present system, the variation of the total free energy of a crystal for small deformations is[51]

$$F_{el} = \frac{1}{2} u_{ij} K_{ijkl} u_{kl} \tag{1}$$

where K_{ijkl} is a tensor of rank four, called the elastic modulus tensor ($i, j, k, l = 1, 2,$ or 3) and u_{ij} is the strain tensor. The elastic modulus tensor for a crystal in terms of the strain tensor is given by

$$K_{ijkl} = \left.\frac{\partial^2 F_{el}}{\partial u_{ij}\partial u_{kl}}\right|_{\mathbf{u}=0} \tag{2}$$

where $\mathbf{u} = 0$ denotes a strain tensor with zero components. For a tetragonal symmetry with a preferred z-axis, K_{ijkl} contains just six independent nonzero components. Under the transformation between x and y axis directions, the general expression for the elastic free energy in the tetragonal system is given by[51]

$$\begin{aligned} F_{el} = {} & \frac{1}{2}K_{11}(u_{xx}^2 + u_{yy}^2) + \frac{1}{2}K_{33}u_{zz}^2 \\ & + K_{13}(u_{xx}u_{zz} + u_{yy}u_{zz}) + K_{12}u_{xx}u_{yy} \\ & + 2K_{66}u_{xy}^2 + 2K_{44}(u_{xz}^2 + u_{yz}^2) \end{aligned} \tag{3}$$

For the lamellar structure perpendicular to the z-axis, deformations along the x- or y-axis directions (parallel to the lamellar structure) have no effect on the free energy. Thus, the elasticity free energy for a lamellar structure reduces to[42]

$$F_{el} = \frac{1}{2}[K_{33}u_{zz}^2 + 4K_{44}(u_{yz}^2 + u_{xz}^2)] \tag{4}$$

In the following, the SCFT calculation for $A(BC)_n$ multiblock copolymer melts with volume V is introduced.[48] The free energy per chain can be written as

$$\begin{aligned} \frac{F}{nk_BT} = {} & -\ln\left(\frac{Q}{V}\right) + \frac{1}{V}\int d\mathbf{r}\left\{\sum_{\substack{I,J=A,B,C \\ I\neq J}} \frac{1}{2}\chi_{IJ}N\varphi_I(\mathbf{r})\varphi_J(\mathbf{r})\right. \\ & \left. - \sum_{I=A,B,C}\omega_I(\mathbf{r})\varphi_I(\mathbf{r}) - \xi(\mathbf{r})\left(1 - \sum_{I=A,B,C}\varphi_I(\mathbf{r})\right)\right\} \end{aligned} \tag{5}$$

where χ_{IJ} is the Flory−Huggins parameter between different species I and J. Q is the partition function of a single chain in the effective chemical potential field $\omega_I(\mathbf{r})$ ($I = A, B, C$) in terms of propagators $q(\mathbf{r},s)$ and $q^+(\mathbf{r},s)$. The spatial coordinate $\mathbf{r}$ is rescaled by R_g, where $R_g^2 = a^2N/6$. The contour length is parametrized with variable s, which starts from one end ($s = 0$) to the other ($s = 1$). The propagators $q(\mathbf{r},s)$ and $q^+(\mathbf{r},s)$ satisfy following modified diffusion equations:

$$\begin{aligned} \frac{\partial q(\mathbf{r},s)}{\partial s} &= [R_g^2\nabla^2 - \omega_{\theta(s)}(\mathbf{r})]q(\mathbf{r},s) \\ -\frac{\partial q^+(\mathbf{r},s)}{\partial s} &= [R_g^2\nabla^2 - \omega_{\theta(s)}(\mathbf{r})]q^+(\mathbf{r},s) \end{aligned} \tag{6}$$

The initial conditions of eq 6 are $q(\mathbf{r},0) = 1$ and $q^+(\mathbf{r},0) = 1$, respectively. $\theta(s)$ is used to specify the segment type along the copolymer chain, subject to $(0 \le i < n)$

$$\theta(s) = \begin{cases} A & \text{if } 0 < s < f_A \\ B & \text{if } f_A + i(\Delta f_B + \Delta f_C) < s < f_A + i(\Delta f_B + \Delta f_C) + \Delta f_B \\ C & \text{if } f_A + i(\Delta f_B + \Delta f_C) + \Delta f_B < s < f_A + (i+1)(\Delta f_B + \Delta f_C) \end{cases} \tag{7}$$

where f_A is the volume fractions of A block and $\Delta f_B = \Delta f_C = (1 - f_A)/2n$, which denotes the volume fractions of B and C block in each BC block. The partition function, Q, for an unconstrained chain is evaluated by summing over all possible position $\mathbf{r}$ of the sth segment, given by $Q = \int d\mathbf{r}\, q(\mathbf{r},s)q^+(\mathbf{r},s)$. The segment densities $\varphi_A(\mathbf{r})$, $\varphi_B(\mathbf{r})$, and $\varphi_C(\mathbf{r})$ are

$$\varphi_A(\mathbf{r}) = \frac{V}{Q}\int_0^{f_A} ds\, q(\mathbf{r},s)q^+(\mathbf{r},s) \tag{8}$$

$$\varphi_B(\mathbf{r}) = \frac{V}{Q}\sum_{i=0}^{n-1}\int_{f_A + i(\Delta f_B + \Delta f_C)}^{f_A + i(\Delta f_B + \Delta f_C) + \Delta f_B} ds\, q(\mathbf{r},s)q^+(\mathbf{r},s) \tag{9}$$

dx.doi.org/10.1021/ma2014035 |Macromolecules 2011, 44, 8314–8323

$$\varphi_C(\mathbf{r}) = \frac{V}{Q}\sum_{i=0}^{n-1}\int_{f_A+i(\Delta f_B+\Delta f_C)+\Delta f_B}^{f_A+(i+1)(\Delta f_B+\Delta f_C)} \mathrm{d}s\, q(\mathbf{r},s)q^+(\mathbf{r},s) \tag{10}$$

The linear elastic moduli for $A(BC)_n$ multiblock copolymer melts in hierarchical lamellar state can be calculated as follows.[47] We first numerically calculate the equilibrium free energy of $A(BC)_n$ multiblock copolymers using eq 5. Then, we change the size or shape of the simulation box to slightly deform the systems from the equilibrium structures, leading to a series of free energies of the deformed lamellar structure. In these calculations, the real-space algorithm for SCFT introduced by Drolet and coworkers was adopted for searching the equilibrium or metastable states.[52,53] By constructing the relation of free energy versus the relative deformation, the elastic moduli can be finally evaluated by taking the second derivative of the SCFT energy with respect to the relative deformation.[54] To yield the extension and shear moduli, we use two ways to deform the system: an extension/compression, which yields K_{33}, and a simple shear, which yields K_{44}. Regarding the extension/compression, the box is extended or compressed by a small change in a direction perpendicular to the lamella, and the free energy is calculated in a rectilinear grid of evaluation points. For the shearing case, however, a nonorthogonal coordinate system is used to calculate the free energy.[55−57]

In order to understand the physical origin of the enhancements in the mechanical properties for the multiblock copolymers, the free energy of SCFT is separated into several physically relevant contributions. Here, the free energy per multiblock copolymer (in units of k_BT) is decomposed as[58]

$$\begin{aligned} F &= U - TS \\ &= \sum_{\substack{I,J=A,B,C \\ I\neq J}} \frac{1}{2}U_{IJ} - T(S_E + S_A + S_{BC}) \end{aligned} \tag{11}$$

where U and S are the internal energy and entropy contributions to free energy, respectively. S_E is the translation entropy of one point of the molecule ($s = f_A$). S_A and S_{BC} are the conformational entropy of A block and BC blocks. Using the standard Gaussian model and SCFT, the corresponding components of the free energy can be written as

$$U_{IJ} = \frac{\chi_{IJ}N}{V}\int \mathrm{d}\mathbf{r}\, \varphi_I(\mathbf{r})\varphi_J(\mathbf{r}) \quad I,J = A,B,C \tag{12}$$

$$-TS_E = \frac{1}{V}\int \mathrm{d}\mathbf{r}\, \rho_E(\mathbf{r}) \ln \rho_E(\mathbf{r}) \tag{13}$$

$$-TS_A = -\frac{1}{V}\int \mathrm{d}\mathbf{r}\, [\rho_E(\mathbf{r}) \ln q(\mathbf{r},f_A) + \omega_A(\mathbf{r})\varphi_A(\mathbf{r})] \tag{14}$$

$$-TS_{BC} = -\frac{1}{V}\int \mathrm{d}\mathbf{r}\, [\rho_E(\mathbf{r}) \ln q^+(\mathbf{r},f_A) + \omega_B(\mathbf{r})\varphi_B(\mathbf{r}) + \omega_C(\mathbf{r})\varphi_C(\mathbf{r})] \tag{15}$$

where $\rho_E(\mathbf{r}) = Vq(\mathbf{r},f_A)q^+(\mathbf{r},f_A)/Q$.

The values of elastic moduli K_{33} and K_{44} can be obtained by taking the second derivative of the SCFT energy with respect to the relative deformation ε. The calculation can be carried out as

$$\begin{aligned} \frac{\partial^2 F}{\partial \varepsilon^2} = &\sum_{\substack{I,J=A,B,C \\ I\neq J}} \frac{1}{2}\frac{\partial^2 U_{IJ}}{\partial \varepsilon^2} + \frac{\partial^2(-TS_E)}{\partial \varepsilon^2} \\ &+ \frac{\partial^2(-TS_A)}{\partial \varepsilon^2} + \frac{\partial^2(-TS_{BC})}{\partial \varepsilon^2} \end{aligned} \tag{16}$$

The modulus K_{33} can be decomposed into the components

$$K_{33} = \sum_{\substack{I,J=A,B,C \\ I\neq J}} \frac{1}{2}K_{33}^{U_{IJ}} + K_{33}^{S_E} + K_{33}^{S_A} + K_{33}^{S_{BC}} \tag{17}$$

where the components $K_{33}^{U_{IJ}}$, $K_{33}^{S_E}$, $K_{33}^{S_A}$, and $K_{33}^{U_{BC}}$ are identified with the derivative in eq 16. Similarly, the decomposition is suitable for K_{44}.

RESULTS AND DISCUSSION

In the present work, we investigated the effect of hierarchical nanostructure on the elastic properties of $A(BC)_n$ linear multiblock copolymers. The studied molecules consist of a long A homopolymer block and a connected $(BC)_n$ multiblock of n identical repeat BC units. In the calculations, the volume fraction f_A was set as 0.5 and the number of repeat BC units was selected as 2−6. Two important parameters influencing the phase behavior of $A(BC)_n$ copolymer were considered: One is the molecular weight governing the appearance of small-length-scale structures, and the other is $\chi_{AB}N$ (or $\chi_{AC}N$) controlling the number of small-length-scale structures.[59]

1. Enhanced Elastic Properties upon Formation of Small-Length-Scale Structures. In this section, we focused on the effect of the appearance of small-length-scale structures on elastic properties of $A(BC)_n$ multiblock copolymers. The values of $\chi_{AB}N$, $\chi_{BC}N$, and $\chi_{AC}N$ were set to be same, denoted as χN. Therefore, for a given copolymer with fixed interaction strengths, the change of $\chi_{BC}N$ (or $\chi_{AB}N$, $\chi_{AC}N$) can be considered as the change of molecular weight, which is of experimental interests. In addition, the number of repeat BC blocks n was set as 2.

To understand the elastic behavior of $A(BC)_2$ multiblock copolymers, we first studied the influence of χN on nanostructure of the multiblock copolymers. Figure 1 shows several representative density profiles at different stages of separation. The top images in the figures show the corresponding two-dimensional structures. As can been seen from Figure 1a, a weakly segregated lamellar structure was observed when χN = 48. It is clear that large amount of A blocks form A-rich lamellar domains and the BC blocks form a mixed matrix. When χN increases to 64, the $A(BC)_2$ multiblock copolymers self-assemble into parallel lamellae-in-lamellar (**L**-in-**L**) structure which contains a thick A lamella and five thin BCBCB lamellae, as shown in Figure 1b. At higher values of interaction strength χN, a strongly separated lamellae-in-lamellar structure emerges, where the B and C blocks are almost completely segregated from each other to form B and C thin layers (Figure 1c).

dx.doi.org/10.1021/ma2014035 |*Macromolecules* 2011, 44, 8314–8323

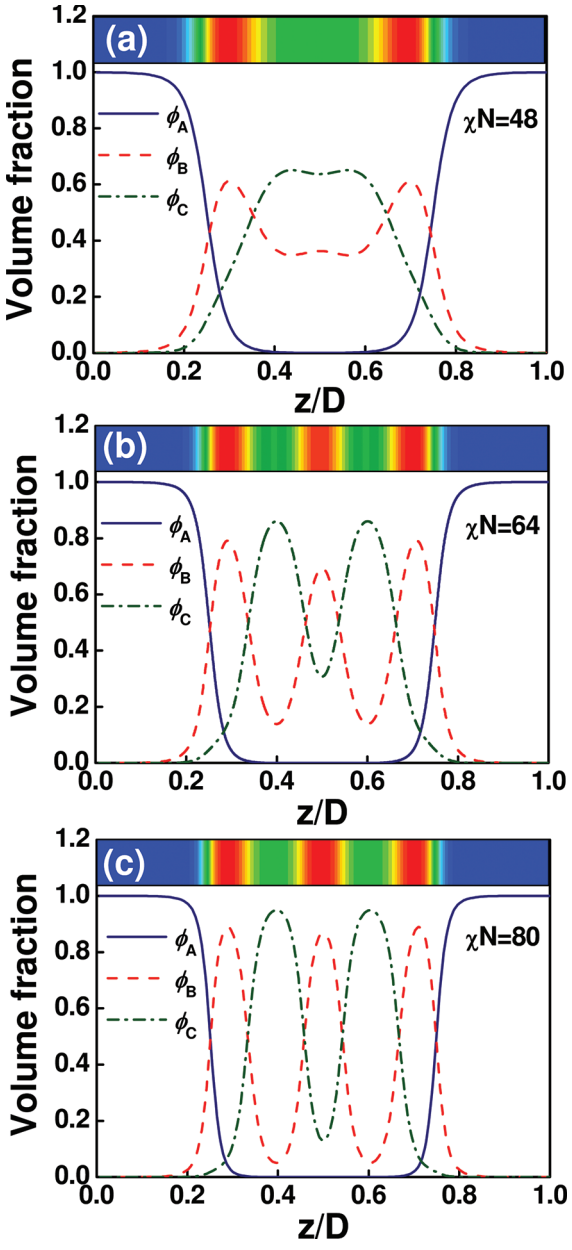

Figure 1. One-dimensional density profiles of A, B, and C blocks of $A(BC)_2$ multiblock copolymers with $f_A = 0.5$ along z-direction at various χN: (a) $\chi N = 48$, (b) $\chi N = 64$, and (c) $\chi N = 80$. The top images show the corresponding two-dimensional structures.

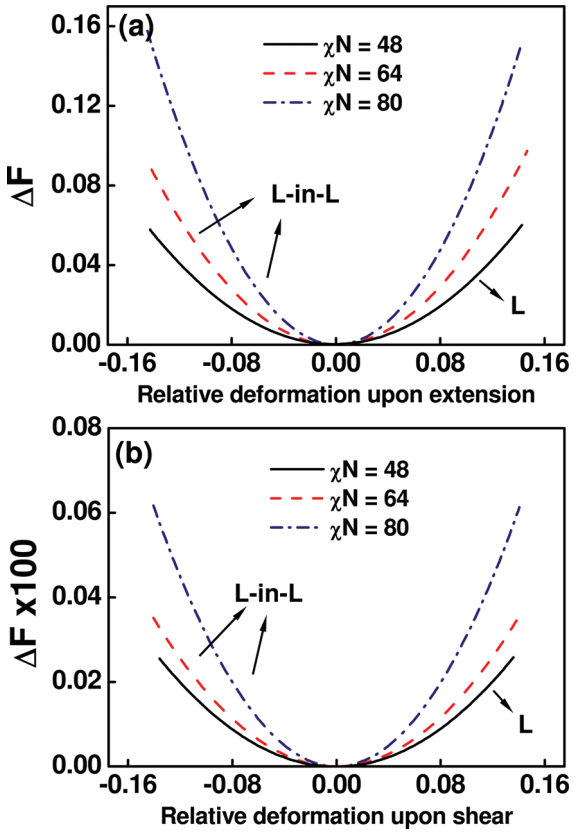

Figure 2. Free energy difference ΔF (in units of k_BT) between the undeformed and deformed structures upon extension/compression (a) and shearing (b) for $A(BC)_2$ multiblock copolymers with various χN. In (a), the negative and positive values of deformation are compression and extension, respectively.

With the evolution of the lamellar phase, the mechanical response undergoes distinct changes. Figure 2 shows the free energy of $A(BC)_2$ multiblock copolymer as a function of the relative extension. The free energies of systems have been zeroed at the equilibrium state, which corresponds to the relative deformation $\varepsilon = 0$. To guarantee the validity of linear elastic theory, the elastic response is within 15% strain. Figures 2a and 2b present the cases of extension/compression and shear deformation, respectively. The change in free energy upon deformation becomes marked as the χN value increases. In comparison with the shear deformation, the variation in free energy upon extension/compression deformation is much larger. As shown in Figure 2, the parabolic character of these curves indicates that the linear elastic theory can be applicable.[42,51] The polynomials are used to fit these curves, and the extension modulus K_{33} and the shear modulus K_{44} can be obtained by taking the second derivative of the free energy change with respect to the relative deformation.

The obtained elastic moduli K_{33} and K_{44} as a function of χN were presented in Figure 3. The moduli variation exhibits a distinct response to the change of χN, which includes three distinct regions. As shown in Figure 3a, within χN range from 32 to 64 (region I), the extension modulus K_{33} increases slightly with increasing χN until it reaches a point where a rapid increase in the slope appears. In the region I, only the general lamellar structure is formed, as shown in Figure 1a. Within χN range of 64−96 (region II), the extension modulus increases remarkably upon increasing χN value, where the structures are gradually transformed from lamella to lamellae-in-lamella with five layers (see Figure 1b). As χN is larger than 96 (region III), the extension modulus K_{33} increases linearly with increasing χN as appeared in region I, where the completely segregated small-length-scale structure is formed in the hierarchical lamellae (see Figure 1c). Comparing with the extension modulus, the shear modulus is much smaller, as shown in Figure 3b. It is also noted that the shear modulus K_{44} vs χN has a great raise over the region II, where the lamella changes into lamellae-in-lamella. With the obtained data of K_{33} and K_{44}, the Young's modulus E upon the structural formation is ready to be evaluated according to $E = [K_{33}(K_{33} + 6K_{44})]/[12(K_{33} + K_{44})]$.[42] The result is shown in

dx.doi.org/10.1021/ma2014035 |*Macromolecules* 2011, 44, 8314–8323

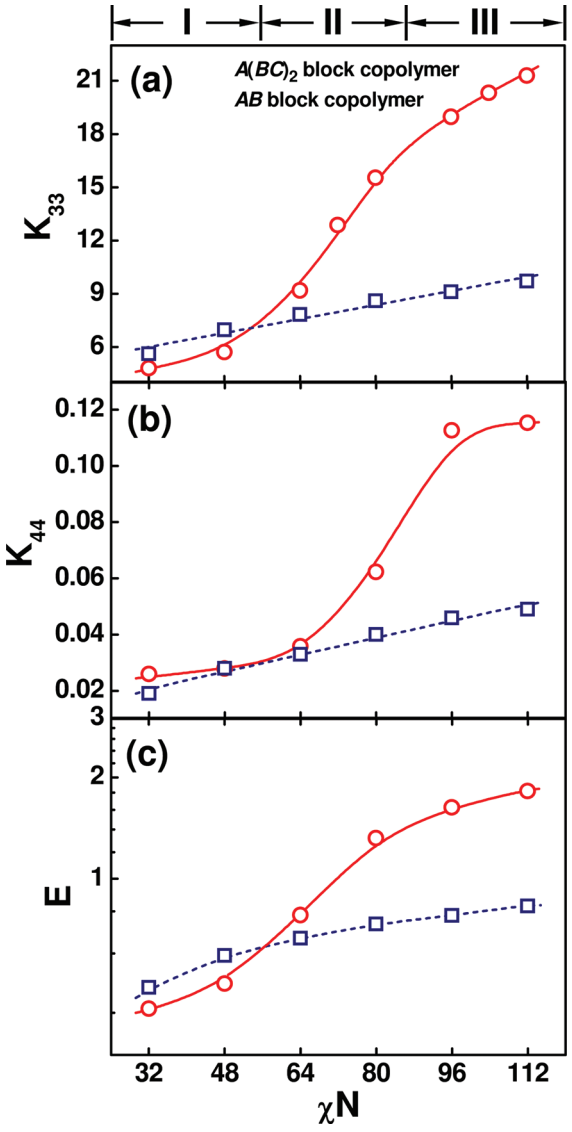

Figure 3. Dimensionless elastic moduli K_{33}, K_{44}, and E as a function of χN for A(BC)$_2$ multiblock copolymers and AB diblock copolymers. The interaction strength in diblock copolymers is the same as χN.

Figure 3c. The Young's modulus E becomes markedly enhanced when the hierarchical structure is formed.

For a deep understanding of the mechanical properties of the hierarchical structures, we also calculated the K_{33}, K_{44}, and E of an AB diblock copolymer for a comparison. The AB diblock copolymers are incapable of self-assembling into the hierarchical nanostructures. The adopted polymerization degree is the same as that of A(BC)$_2$ copolymers. In Figure 3a−c, the blue lines represent the extension, shear, and Young's moduli of AB diblock copolymers, respectively. The extension or shear modulus increase linearly with increasing χN. In region I, the moduli of both AB and A(BC)$_2$ block copolymers are similar. However, in regions II and III, the AB block copolymer displays a constant increase tendency of the modulus, showing a weaker elastic properties as compared to the A(BC)$_2$ copolymers. According to these results, we can conclude that the A(BC)$_2$ multiblock copolymers with lamellae-in-lamellar structure have apparent advantages over the simple diblock copolymers in mechanical properties.

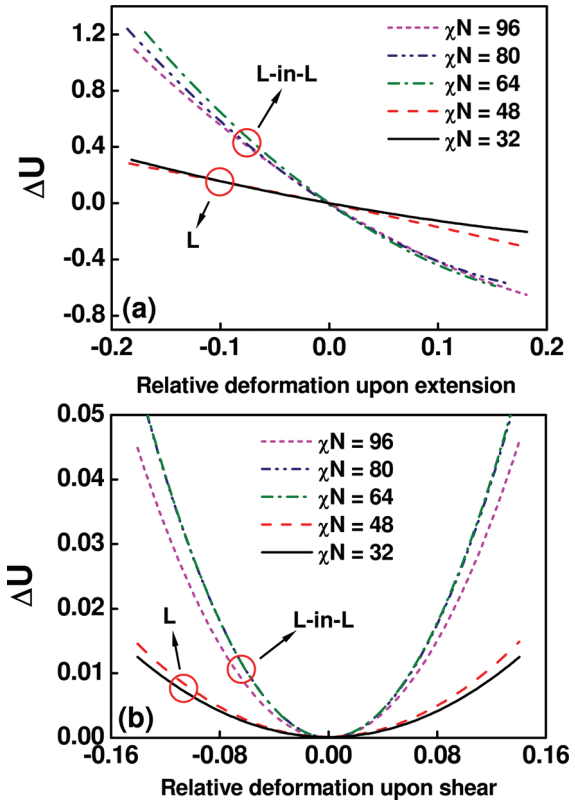

Figure 4. Difference of internal energy ΔU (in units of k_BT) versus the relative deformation under extension/compression (a) and shear (b) for different structures of A(BC)$_2$ multiblock copolymers.

Some experimental observations are available in the literature for supporting our predictions. Bates et al. have recently studied the viscoelastic and mechanical properties of several samples of CECEP hexablock copolymer which consists of a long poly(ethylene-*alt*-polylene) (P) tail block and five short polycyclohexylethylene (C) and polyethylene (E) blocks.[24] Phase transition from bicontinuous-like structure to hierarchical lamellar structure takes place with increasing molecular weight, which is proportional to the degree of polymerization N. The mechanical properties were evaluated by tensile testing. The results demonstrated that the mechanical properties of these materials mainly depend on the formation of the substructure. Remarkable improvements of the mechanical property of these materials were displayed upon the formation of the hierarchical structures. They suggested that it is due to the intrinsic toughness of the microphase-separated CECEC substructures in the lamellae-in-lamellar structures. In our simulations, the mechanical properties are highly improved, when hierarchical lamellar structures are formed with increasing the interaction χN (the degree of polymerization N at fixed χ value). These results are qualitatively consistent with the experimental findings.

It should be noted that the hierarchical structure in experiments is perpendicular **L**-in-**L** while in simulations is parallel **L**-in-**L**. According to our previous work as well as Li et al., the sequence of the interaction strengths plays a determining role in formation of hierarchical structures with different arrangements.[48,60] The perpendicular **L**-in-**L** can be formed when $\chi_{AC} < \chi_{AB}$ and χ_{BC} is significantly large in A(BC)$_n$ multiblock copolymers. The difference between the simulations and experiments

Table 1. Components of Dimensionless K_{33} (a) and K_{44} (b) for Lamellar Structures of A(BC)$_2$ Multiblock Copolymers with Various χN

(a)	χN	K_{33}	K_{33}^{U}	$K_{33}^{U_{AB}+U_{AC}}$	$K_{33}^{U_{BC}}$	K_{33}^{S}	$K_{33}^{S_E}$	$K_{33}^{S_A}$	$K_{33}^{S_{BC}}$
L	32	4.879	3.111	3.873	−0.762	1.768	−0.659	1.273	1.154
	48	5.721	−1.215	3.057	−4.272	6.936	−0.419	1.785	5.570
L-in-**L**	64	8.978	21.182	4.797	16.385	−12.204	−1.334	3.114	−13.984
	80	15.377	16.714	3.826	12.888	−1.337	−1.247	3.166	−3.256
	96	18.022	13.836	3.628	10.208	4.186	−1.201	3.559	1.828
(b)	χN	K_{44}	K_{44}^{U}	$K_{44}^{U_{AB}+U_{AC}}$	$K_{44}^{U_{BC}}$	K_{44}^{S}	$K_{44}^{S_E}$	$K_{44}^{S_A}$	$K_{44}^{S_{BC}}$
L	32	0.0264	1.253	1.526	−0.273	−1.227	−0.577	−0.301	−0.349
	48	0.0279	1.477	1.760	−0.283	−1.449	−0.775	−0.350	−0.324
L-in-**L**	64	0.0358	5.618	1.876	3.742	−5.582	−0.918	−0.728	−3.936
	80	0.0623	5.576	2.455	3.121	−5.514	−0.880	−0.983	−3.651
	96	0.113	4.605	2.580	2.025	−4.492	−0.857	−1.108	−2.527

can be ascribed to the different interaction parameters in the two systems. In the simulations, the χ_{AC} is set equal to χ_{AB}, and thus a parallel **L**-in-**L** was formed. While in experiments, the sequence of interaction strength is $\chi_{AC} < \chi_{AB} \ll \chi_{BC}$, and the perpendicular **L**-in-**L** was observed.

At present, direct theoretical treatments of the perpendicular structure is more complicated. For example, eq 3 cannot be simplified as eq 4, and more terms of eq 3 should remain in the simplification of eq 3 to eq 4. However, for the parallel structure, eq 4 is applicable since the free energy only changes in the direction normal to the lamellae at large length scale. For these reasons, in the present work we consider the parallel **L**-in-**L** structure as a model for understanding the effects of hierarchical structure on the mechanical properties. Despite the difference in the two structures, the enhancements of the mechanical properties upon the formation of the hierarchical structure can be same. In addition, as indicated by Bates et al., the arrangement of the small-length-scale structures (perpendicular, parallel, or else) may have less marked effect on the mechanical properties, and the appearance of the small-length-scale structures should play an important role in improving the mechanical properties.[24] Therefore, the experiments well support our predictions.

We also emphasize that all these SCFT calculations were performed in the melt state. SCFT has difficulty in predicting the elastic properties of a nonmelt system due to its own shortcoming. However, the results obtained from the melt state could be applicable to the situation in the nonmelt system.[47] Although the observation reported by Fleury and Bates was carried out in a nonmelt system, extending the results obtained from the melt state to nonmelt situation would be a reasonable argument. Our theoretical calculations not only predict the general feature of the hierarchical structure influence on mechanical properties but also predict the phenomena that have not been observed yet.

To find out the origin of the dramatic increase in the elastic moduli upon the formation of hierarchical nanostructures, we decomposed the free energy into several parts according to eqs 11−15. One is the contribution of internal energy U, and the other arises from the contribution of conformational entropy $-TS$, which includes the translational entropy S_E and conformational entropies of A block S_A and BC block S_{BC}. Figure 4 shows the typical results obtained for internal energy contributions to the total free energy change for extension/compression and shear of the A(BC)$_n$ linear multiblock copolymers with n = 2.

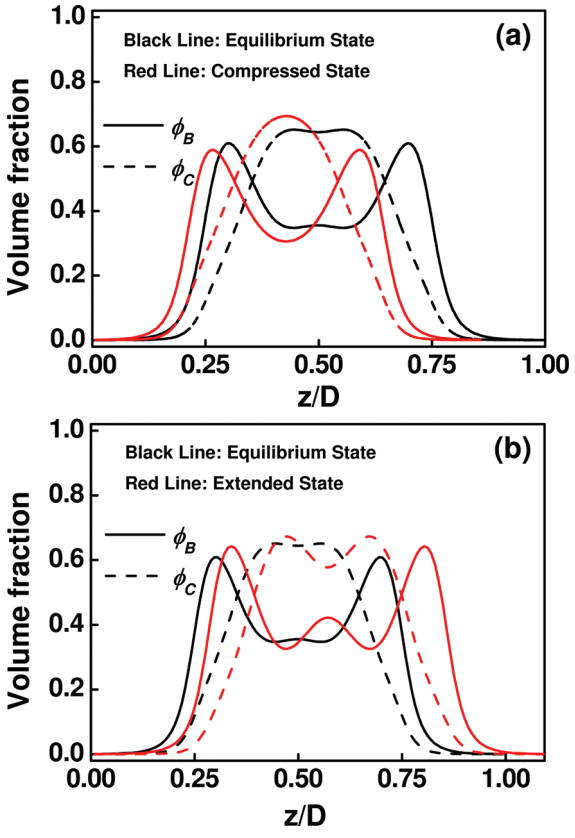

Figure 5. One-dimensional density profiles of B and C blocks of A(BC)$_2$ multiblock copolymers at χN = 48. The black lines correspond to the equilibrium state, and red lines correspond to the states under compression (a) and extension (b).

The contribution of internal energy change to the total free energy change of the multiblock copolymer at χN = 32 and 48 corresponds to the general lamellar phase, and the curves of internal energy components at χN = 64, 80, and 96 correspond to the **L**-in-**L** phase.

Taking the second derivative of internal energy and entropy changes with respect to the relative deformation, we obtained the moduli contributed from the internal energy and entropy for

dx.doi.org/10.1021/ma2014035 |*Macromolecules* 2011, 44, 8314–8323

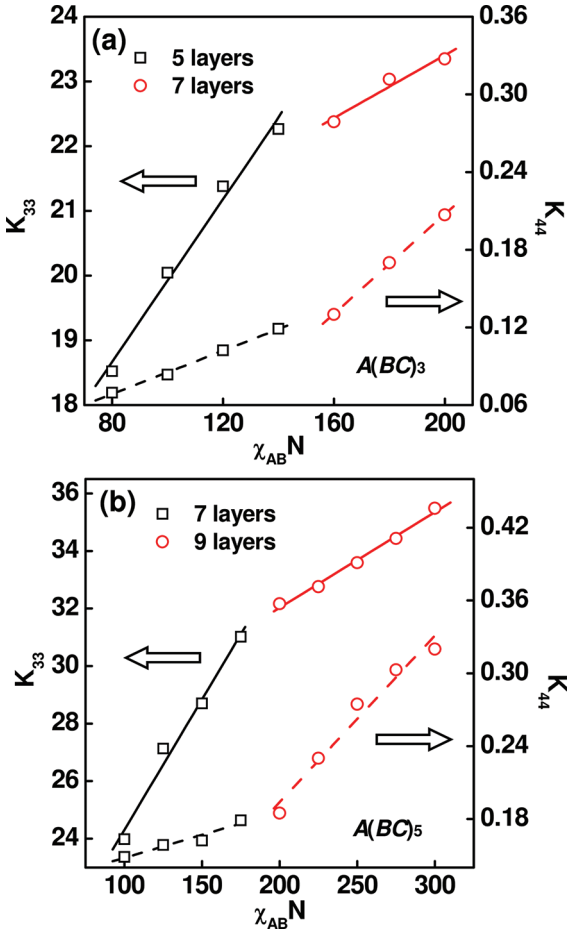

Figure 6. Dimensionless elastic moduli K_{33} and K_{44} as a function of $\chi_{AB}N$ for A(BC)$_n$ multiblock copolymer with n = 3 (a) and n = 5 (b). The solid and dashed lines represent the moduli K_{33} and K_{44}, respectively.

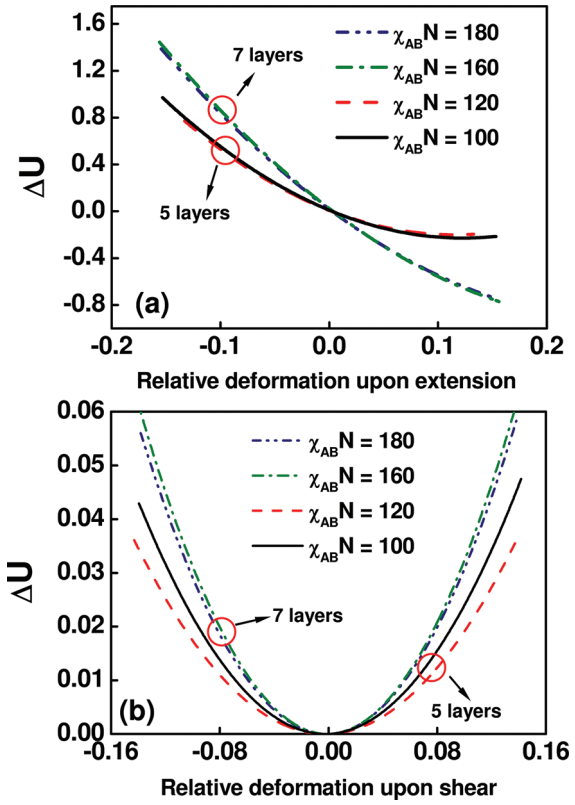

Figure 7. Difference of internal energy ΔU (in units of k_BT) versus the relative deformation under extension/compression (a) and shear (b) for **L**-in-**L** with 5 and 7 layers of A(BC)$_3$ multiblock copolymers.

A(BC)$_2$ multiblock copolymers with various χN values, which are listed in Table 1. K_{33} (K_{44}) is the total extension (shear) modulus and is the sum of internal energy contributions K_{33}^U (K_{44}^U) and entropy contributions K_{33}^S (K_{44}^S). Herein, the internal energy contributions K_{33}^U (K_{44}^U) were further divided into $K_{33}^{U_{AB}+U_{AC}}$ ($K_{44}^{U_{AB}+U_{AC}}$) contributed from the interaction between A and BC blocks and $K_{33}^{U_{BC}}$ ($K_{44}^{U_{BC}}$) contributed from the interaction between B and C blocks, while the entropy contributions K_{33}^S (K_{44}^S) was decomposed into $K_{33}^{S_E}$ ($K_{44}^{S_E}$), $K_{33}^{S_A}$ ($K_{44}^{S_A}$), and $K_{33}^{S_{BC}}$ ($K_{44}^{S_{BC}}$) contributed respectively from E junction translation, A block conformation, and BC block conformation. As can be seen from Table 1a, both the lamellar and **L**-in-**L** structures have the same feature of the contributions of the internal energy and the conformational entropy to the total moduli. In each type of structure (lamella or **L**-in-**L**), the extension modulus contributed from internal energy, $K_{33}^{S_{BC}}$, is inversely proportional to the effective interaction χN, while the modulus contributed from conformational entropy, $K_{33}^{S_{BC}}$, becomes larger with increasing χN. The variations of $K_{33}^{U_{AB}+U_{AC}}$, $K_{33}^{S_A}$, and K_{33}^{E} are relatively smaller. It is further noted that the $K_{33}^{U_{BC}}$ increases remarkably when the transition from lamella to **L**-in-**L** takes place. The decrease in $K_{33}^{S_{BC}}$ was also observed as lamella transforms to **L**-in-**L** but cannot prevent the increase in the extension modulus, since the variations of $K_{33}^{U_{BC}}$ dominate over $K_{33}^{S_{BC}}$. Therefore, the increase in $K_{33}^{U_{BC}}$ is the main driving force to make the materials tough, when the hierarchical structures form. Similarly, Table 1b displays the internal energy and entropy contributions to the shear modulus, which resembles the situation of extension modulus. As can be seen, the $K_{44}^{U_{BC}}$ contributed from internal energy and $K_{44}^{S_{BC}}$ contributed from conformational entropy of BC blocks are mainly responsible for the change of shear modulus when the phase transition from lamella to **L**-in-**L** occurs, while the variations of $K_{44}^{U_{AB}+U_{AC}}$, $K_{44}^{S_A}$, and $K_{44}^{S_E}$ are relatively smaller. Because the $K_{33}^{U_{BC}}$ ($K_{44}^{U_{BC}}$) and $K_{33}^{S_{BC}}$ ($K_{44}^{S_{BC}}$) are directly related to the BC domains, we can conclude that the appearance of small-length-scale structures have a crucial contribution to the enhancement of the modulus.

Since the internal energy U_{BC} and conformational entropy S_{BC} play important roles in determining the enhancement of K_{33} and K_{44} upon the formation of **L**-in-**L** structures, we further conducted a detailed analysis of these two contributors in K_{33} for an example. Before the formation of hierarchical structures, the A(BC)$_n$ multiblock copolymers self-assemble into general **L** structures, where B and C blocks are mixed into one domain. In this structure, the conformational entropy is gained through increasing unfavorable enthalpy. Therefore, the **L** structures have a tendency of decreasing internal energy by increasing entropic losses through a distortion of the systems. In other words, U_{BC} helps deforming the system in **L** structures. This can be confirmed by Figure 5, where the densities of B (solid) and C (dash) blocks are plotted upon extension and compression. The black and red curves correspond to density profiles at equilibrium and under distortion, respectively. As shown in Figure 5a, when the

dx.doi.org/10.1021/ma2014035 |*Macromolecules* 2011, 44, 8314–8323

Table 2. Components of Dimensionless K_{33} (a) and K_{44} (b) for L-in-L Structures with 5 and 7 Layers of $A(BC)_3$ Multiblock Copolymers with Various $\chi_{AB}N$

(a)	$\chi_{AB}N$	K_{33}	K_{33}^{U}	$K_{33}^{U_{AB}+U_{AC}}$	$K_{33}^{U_{BC}}$	K_{33}^{S}	$K_{33}^{S_E}$	$K_{33}^{S_A}$	$K_{33}^{S_{BC}}$
5 layers	100	20.078	33.003	9.972	23.031	−12.925	−2.792	3.035	−13.168
	120	21.388	32.872	8.783	24.089	−11.484	−2.586	3.382	−12.280
	140	22.347	32.015	6.701	25.314	−9.668	−1.662	3.512	−11.518
7 layers	160	22.467	24.671	3.654	21.017	−2.204	−1.237	4.543	−5.510
	180	23.089	22.053	1.301	20.752	1.036	−1.253	4.818	−2.529
	200	23.437	21.575	1.068	20.507	1.862	−1.161	4.862	−1.839
(b)	$\chi_{AB}N$	K_{44}	K_{44}^{U}	$K_{44}^{U_{AB}+U_{AC}}$	$K_{44}^{U_{BC}}$	K_{44}^{S}	$K_{44}^{S_E}$	$K_{44}^{S_A}$	$K_{44}^{S_{BC}}$
5 layers	100	0.0837	4.574	2.075	2.499	−4.490	−0.944	−0.468	−3.078
	120	0.0977	3.650	1.939	1.711	−3.552	−0.886	−0.320	−2.346
	140	0.119	3.222	1.906	1.316	−3.103	−0.851	−0.225	−2.027
7 layers	160	0.131	6.358	1.765	4.593	−6.227	−0.884	−1.421	−3.922
	180	0.168	5.990	1.680	4.310	−5.822	−0.873	−1.323	−3.626
	200	0.207	5.875	1.662	4.213	−5.668	−0.864	−1.380	−3.424

system is compressed, the density of B blocks in the center of domain becomes lower, giving rise to a decrease of internal energy. In addition, when the system is extended, the B blocks in the center of domain are separated from C blocks (Figure 5b), leading to a decrease of internal energy. On the other hand, the entropic losses of B and C blocks increase upon extension/compression due to frustration of chain under distortion. It means that S_{BC} becomes unfavorable for deformed system. As a result, the modulus contributed from the internal energy and entropy change of BC blocks is negative and positive, respectively, as shown in Table 1a.

For **L**-in-**L** structures, however, the BC blocks split into five thin domains, which leads to a great decrease of internal energy between B and C blocks. Therefore, the internal energy tends to resist the deformation. Meanwhile, the entropic losses of BC blocks increase with decreasing the BC internal energy and thus help deform the system. This is the reason that the modulus contributed from BC enthalpy and entropy is respectively positive and negative, which exhibits an opposite case of **L** structures. According to the above arguments, the BC domains of $A(BC)_n$ multiblock copolymers exhibit entropy elasticity (positive $K_{33}^{S_{BC}}$) at **L** state and enthalpy elasticity (positive $K_{33}^{U_{BC}}$) at **L**-in-**L** state.

2. Effect of Number of Small-Length-Scale Structures on Elastic Properties. In this section, we extended our analysis to the elastic properties of **L**-in-**L** with different number of small-length-scale layers. In the previous work, we have learned that a change of $\chi_{AB}N$ (or $\chi_{AC}N$) can give rise to a change of the number of small-length-scale structures.[48,59] Therefore, we first carried out a study of different equilibrium structures at different $\chi_{AB}N$, where the $\chi_{AC}N$ was set equal to $\chi_{AB}N$ and the $\chi_{BC}N/n$ value was fixed as 40. The results were obtained as follows. When the number of repeating BC blocks n is 3, $A(BC)_3$ multiblock copolymers self-assemble into **L**-in-**L** structures with 5 and 7 internal layers at lower and higher $\chi_{AB}N$, respectively. As for n = 5, $A(BC)_5$ multiblock copolymers self-assemble into **L**-in-**L** structures with 7 or 9 internal layers at different $\chi_{AB}N$. The change of small-length-scale layers caused by the change of $\chi_{AB}N$ can also lead to a change of mechanical properties.

SCF calculation reveals that the $A(BC)_n$ multiblock copolymers exhibit different mechanical responses when they take different hierarchical structures with various number of small-length-scale layers. Figure 6a shows the elastic moduli K_{33} and K_{44} as a function of $\chi_{AB}N$ at n = 3. Over the range of $\chi_{AB}N$ from 80 to 200, $A(BC)_3$ multiblock copolymers self-assemble into the hierarchical structures with 5 and 7 internal BC layers, respectively. Increasing the value of $\chi_{AB}N$ for each stable structure gives rise to a linear increase in extension and shear modulus (K_{33} and K_{44}). However, in the two different hierarchical structures, the increase in elastic moduli exhibits different trend from each other. For **L**-in-**L** structure with 5 layers, the extension modulus K_{33} (shear modulus K_{44}) increases more remarkably (moderately) relative to the nanostructure with 7 layers. The situation can be extended to other cases, for example, n = 5. The results for n = 5 case is shown in Figure 6b. Over the range of $\chi_{AB}N$ from 100 to 300, hierarchical structures with 7 and 9 internal layers were observed. When 7-layered structure transforms into 9-layered structure, the slope of K_{33} change becomes flatter and the slope of K_{44} change becomes steeper, which means that the materials with hierarchical nanostructures containing more small-length-scale layers exhibit more enhanced shear modulus. It is noted that the multiblock copolymers with n = 4 and 6 show the same dependence of the mechanical properties on the hierarchical structure as those of n = 2, 3, and 5. For example, K_{33} increases linearly with increasing $\chi_{AB}N$. For the sake of simplicity, the results of n = 4 and 6 are not shown.

The effect of the number of small-length-scale layers on the elastic properties can be further understood by analyzing the contributions from internal energy and entropy changes. Figure 7a shows the contributions of internal energy change ΔU to the total free energy change as a function of the relative deformation upon the extension/compression for $A(BC)_3$ multiblock copolymer. When $\chi_{AB}N$ = 100 and 120, corresponding to the structure with 5 *BC* layers, the curves of the contribution of internal energy change to the total free energy change are almost overlapped with each other, and so do the curves when $\chi_{AB}N$ = 160 and 180, corresponding to the structure with 7 BC layers. For each type of the structures, the contribution of internal energy change to the total free energy change decreases as $\chi_{AB}N$ increases. Moreover, the internal energy change contribution becomes smaller as more BC internal layers form. Figure 7b shows the contributions of internal energy change to the total free energy

change as a function of the relative deformation upon shear. When the number of small-length-scale layers changes from 5 to 7, the contribution of internal energy change to total free energy change shows an increase. Meanwhile, for each structure with fixed number of small-length-scale layers, the contribution of internal energy change decreases with increasing $\chi_{AB}N$. A similar phenomenon has also been observed for the entropy change contribution to the total free energy change.

More detailed information concerning the moduli contributed from enthalpy and entropy changes is listed in Table 2. The K_{33} (K_{44}) is the sum of $K_{33}^{U_{AB}+U_{AC}}$, $K_{33}^{S_{BC}}$, $K_{33}^{S_E}$, $K_{33}^{S_A}$, and $K_{33}^{S_{BC}}$ ($K_{44}^{U_{AB}+U_{AC}}$, $K_{44}^{U_{BC}}$, $K_{44}^{S_E}$, $K_{44}^{S_A}$, and $K_{44}^{S_{BC}}$). As can be seen from Table 2a, $K_{33}^{U_{AB}+U_{AC}}$, $K_{33}^{U_{BC}}$, and $K_{33}^{S_{BC}}$ are the major factors influencing the moduli of different structures. When the 5-layered structures transform into the 7-layered structures, $K_{33}^{U_{AB}+U_{AC}}$ and $K_{33}^{U_{BC}}$ decrease but $K_{33}^{S_{BC}}$ increases, resulting in a moderate increase in the extension moduli (see Figure 6a). However, the enthalpy and entropy change contributions to shear modulus K_{44} are not the same case, as can be seen in Table 2b. Relative to the 5-layered structures, $K_{44}^{U_{BC}}$ becomes much larger and $K_{44}^{U_{AB}+U_{AC}}$ becomes smaller in 7-layered structures. Meanwhile, the negative $K_{44}^{S_A}$ and $K_{44}^{S_{BC}}$ become smaller. These effects accelerate the increase of K_{44} in 7-layered structure, as can be seen in Figure 6a.

We further analyzed the mechanism behind the variation of K_{33} and K_{44} in the transformation from 5-layered to 7-layered structures. Because the shear moduli are much smaller than the extension moduli, here we mainly focused on the cases of K_{33}. Since the interfacial width of hierarchical structures is less affected upon extension/compression, the decrease in $K_{33}^{U_{AB}+U_{AC}}$ and $K_{33}^{U_{BC}}$ with increasing the number of small-length-scale structures can be explained according to the equation $K_{33}^{U} = (\partial^2 U/\partial\varepsilon^2)|_{\varepsilon=0} = 2\alpha/d^*$, where α is a constant and d^* is the equilibrium domain size.[43] This equation indicates that K_{33}^{U} is inversely proportional to the domain size. As the small-length-scale structure changes from 5 layers to 7 layers, the domain size of the large-length-scale lamella becomes larger and so does the thickness of BC internal layers at small length scale. As a consequence, both $K_{33}^{U_{AB}+U_{AC}}$ and $K_{33}^{U_{BC}}$ decrease when more small-length-scale structures are formed. On the other hand, the conformational entropy of BC blocks favors the deformed **L**-in-**L** structures because of the chain stretching nature in microphase-separated state. When the hierarchical structure changes from 5-layered to 7-layered structure, the entropic losses of BC blocks decrease due to the increased conformational number.[48,59] This means that BC blocks become less inclined to deform the system. As a result, the modulus $K_{33}^{S_{BC}}$ contributed from conformational entropy of BC blocks increases a lot with increasing the number of small-length-scale layers.

As far as we know, this is the first example of the investigation on the mechanical properties of hierarchical structures using a model of $A(BC)_n$ multiblock copolymers. The obtained results indicate that the hierarchically structured materials show highly enhanced mechanical properties relative to the general materials with single-periodic nanostructures. The results are found to be in good qualitative agreement with the experimental observations. The parallel **L**-in-**L** structure can be regarded as a simple realized model of the hierarchical structures with lower level. It resembles biomaterials with multiple hierarchies of self-similar structures, such as staggered nanostructure of bone. Our studies are of both theoretical means and practical applications. In practice, the observed results may provide useful information for designing and fabricating advanced materials.

CONCLUSION

We utilized real-space self-consistent field theory to calculate the elastic modulus of $A(BC)_n$ multiblock copolymer in hierarchical **L**-in-**L** structures. The extension, shear, and Young's moduli have been examined as functions of interaction strengths, in the cases of different lamellar phases. The appearance of the small-length-scale structure in **L**-in-**L** gives rise to the enhancement of mechanical properties significantly. The increase of extension and shear modulus in **L**-in-**L** is mainly due to the increased internal energy change contribution inherent in small-length-scale structures. On the other hand, the number of small-length-scale layers also plays a significant role in determining the mechanical properties of the $A(BC)_n$ multiblock copolymers. For the **L**-in-**L** structures containing more small-length-scale layers, the extension modulus becomes less sensitive to the change of interaction strength, but the shear modulus shows more sensitive. These distinct mechanical responses of hierarchical structures are mainly contributed from the interplay of internal energy and conformational entropy of BC blocks.

AUTHOR INFORMATION

Corresponding Author

*Tel: +86-21-64253370. Fax: +86-21-64251644. E-mail: jlin@ecust.edu.cn or jplinlab@online.sh.cn.

ACKNOWLEDGMENT

This work was supported by National Natural Science Foundation of China (50925308). Support from projects of Shanghai municipality (09XD1401400, 0952 nm05100, 08DZ2230500, and B502) is also appreciated.

REFERENCES

(1) Jäger, I.; Fratzl, P. *Biophys. J.* **2000**, *79*, 1737–1746.
(2) Fratzl, P.; Gupta, H. S.; Paschalis, E. P.; Roschger, P. *J. Mater. Chem.* **2004**, *14*, 2115–2123.
(3) Autumn, K.; Liang, Y. A.; Hsieh, S. T.; Zesch, W.; Chan, W. P.; Kenny, T. W.; Fearing, R.; Full, R. J. *Nature* **2000**, *405*, 681–684.
(4) Menig, R.; Meyers, M. H.; Meyers, M. A.; Vecchio, K. S. *Mater. Sci. Eng., A* **2001**, *297*, 203–211.
(5) Weiner, S.; Wagner, H. D. *Annu. Rev. Mater. Sci.* **1998**, *28*, 271–298.
(6) Qin, Z.; Kreplak, L.; Buehler, M. J. *PLoS ONE* **2009**, *4*, e7294.
(7) Hanski, S.; Houbenov, N.; Ruokolainen, J.; Chondronicola, D.; Iatrou, H.; Hadjichristidis, N.; Ikkala, O. *Biomacromolecules* **2006**, *7*, 3379–3384.
(8) Tung, S.-H.; Kalarickal, N. C.; Mays, J. W.; Xu, T. *Macromolecules* **2008**, *41*, 6453–6462.
(9) Iatrou, H.; Frielinghaus, H.; Hanski, S.; Ferderigos, N.; Ruokolainen, J.; Ikkala, O.; Richter, D.; Mays, J.; Hadjichristidis, N. *Biomacromolecules* **2007**, *8*, 2173–2181.
(10) Ma, Z.; Yu, H.; Jiang, W. *J. Phys. Chem. B* **2009**, *113*, 3333–3338.
(11) Han, Y.; Jiang, W. *J. Phys. Chem. B* **2011**, *115*, 2167–2172.
(12) Ruokolainen, J.; Mäkinen, R.; Torkkeli, M.; Mäkelä, T.; Serimaa, R.; ten Brinke, G.; Ikkala, O. *Science* **1998**, *280*, 557–560.
(13) Nandan, B.; Lee, C.-H.; Chen, H.-L.; Chen, W.-C. *Macromolecules* **2006**, *39*, 4460–4468.
(14) Masuda, J.; Takano, A.; Nagata, Y.; Noro, A.; Matsushita, Y. *Phys. Rev. Lett.* **2006**, *97*, 098301.
(15) Ikkala, O.; ten Brinke, G. *Science* **2002**, *295*, 2407–2409.
(16) Valkama, S.; Kosonen, H.; Ruokolainen, J.; Haatainen, T.; Torkkeli, M.; Serimaa, R.; ten Brinke, G.; Ikkala, O. *Nature Mater.* **2004**, *3*, 872–876.

(17) Ruokolainen, J.; ten Brinke, G.; Ikkala, O. *Adv. Mater.* **1999**, *11*, 777–780.
(18) Ruotsalainen, T.; Turku, J.; Heikkila, P.; Ruokolainen, J.; Nykanen, A.; Laitinen, T.; Torkkeli, M.; Serimaa, R.; ten Brinke, G.; Harlin, A.; Ikkala, O. *Adv. Mater.* **2005**, *17*, 1048–1052.
(19) Matsushita, Y. *Polym. J.* **2008**, *40*, 177–183.
(20) Matsushita, Y.; Takano, A.; Hayashida, K.; Asari, T.; Noro, A. *Polymer* **2009**, *50*, 2191–2203.
(21) Matsushita, Y. *Macromolecules* **2007**, *40*, 771–776.
(22) Masuda, J.; Takano, A.; Suzuki, J.; Nagata, Y.; Noro, A.; Hayashida, K.; Matsushita, Y. *Macromolecules* **2007**, *40*, 4023–4027.
(23) Fleury, G.; Bates, F. S. *Macromolecules* **2009**, *42*, 1691–1694.
(24) Fleury, G.; Bates, F. S. *Macromolecules* **2009**, *42*, 3598–3610.
(25) Bates, F. S.; Fredrickson, G. H. *Annu. Rev. Phys. Chem.* **1990**, *41*, 525–557.
(26) Bates, F. S.; Fredrickson, G. H. *Phys. Today* **1999**, *52*, 32–38.
(27) Tyler, C. A.; Morse, D. C. *Phys. Rev. Lett.* **2005**, *94*, 208302.
(28) Matsushita, Y.; Nomura, M.; Watanabe, J.; Mogi, Y.; Noda, I.; Imai, M. *Macromolecules* **1995**, *28*, 6007–6013.
(29) Matsen, M. W.; Thompson, R. B. *J. Chem. Phys.* **1999**, *111*, 7139–7146.
(30) Hermel, T. J.; Wu, L.; Hahn, S. F.; Lodge, T. P.; Bates, F. S. *Macromolecules* **2002**, *35*, 4685–4689.
(31) Wu, L.; Lodge, T. P.; Bates, F. S. *Macromolecules* **2004**, *37*, 8184–8187.
(32) Wang, Z.-G. *J. Chem. Phys.* **1994**, *100*, 2298–2301.
(33) Yeung, C.; Shi, A.-C.; Noolandi, J.; Desai, R. C. *Macromol. Theory Simul.* **1996**, *5*, 291–298.
(34) Hamley, I. W. *Phys. Rev. E* **1994**, *50*, 2872–2880.
(35) Pereira, G. G. *J. Chem. Phys.* **2002**, *117*, 1878–1887.
(36) Buxton, G. A.; Balazs, A. C. *J. Chem. Phys.* **2002**, *117*, 7649–7658.
(37) Buxton, G. A.; Balazs, A. C. *Macromolecules* **2005**, *38*, 488–500.
(38) Hong, K. M.; Noolandi, J. *Macromolecules* **1981**, *14*, 727–736.
(39) Matsen, M. W. *Soft Matter* **2006**, *2*, 1048–1056.
(40) Fredrickson, G. H. *Soft Matter* **2007**, *3*, 1329–1334.
(41) Tyler, C. A.; Morse, D. C. *Macromolecules* **2003**, *36*, 3764–3774.
(42) Thompson, R. B.; Rasmussen, K. Ø.; Lookman, T. *J. Chem. Phys.* **2004**, *120*, 3990–3996.
(43) Thompson, R. B.; Rasmussen, K. Ø.; Lookman, T. *Nano Lett.* **2004**, *4*, 2455–2459.
(44) Jiang, Y.; Huang, R.; Liang, H. *J. Chem. Phys.* **2005**, *123*, 124906.
(45) Huang, R.; Jiang, Y.; Liang, H. *ChemPhysChem* **2006**, *7*, 1950–1956.
(46) Maniadis, P.; Lookman, T.; Kober, E. M.; Rasmussen, K. Ø. *Phys. Rev. Lett.* **2007**, *99*, 048302.
(47) Zhang, L.; Lin, J.; Lin, S. *Soft Matter* **2009**, *5*, 173–181.
(48) Wang, L.; Lin, J.; Zhang, L. *Macromolecules* **2010**, *43*, 1602–1609.
(49) Zhu, X.; Wang, L.; Lin, J.; Zhang, L. *ACS Nano* **2010**, *4*, 4979–4988.
(50) Zhang, L.; Lin, J. *Macromolecules* **2009**, *42*, 1410–1414.
(51) Landau, L. D.; Lifshitz, E. M. *Theory of Elasticity*, 3rd ed.; Butterworth-Heinemann: Oxford, 1999.
(52) Drolet, F.; Fredrickson, G. H. *Phys. Rev. Lett.* **1999**, *83*, 4317–4320.
(53) Fredrickson, G. H.; Ganesan, V.; Drolet, F. *Macromolecules* **2002**, *35*, 16–39.
(54) Kossuth, M. B.; Morse, D. C.; Bates, F. S. *J. Rheol.* **1999**, *43*, 167–196.
(55) Tzeremes, G.; Rasmussen, K. Ø.; Lookman, T.; Saxena, A. *Phys. Rev. E* **2002**, *65*, 041806.
(56) Rasmussen, K. Ø.; Kalosakas, G. *J. Polym. Sci., Part B: Polym. Phys.* **2002**, *40*, 1777–1783.
(57) Frigo, M.; Johnson, S. G. *The Fast Fourier Transform in the West 2.1.3*; MIT: Cambridge, MA, 2000 (http://www.fftw.org).
(58) Matsen, M. W.; Bates, F. S. *J. Chem. Phys.* **1997**, *106*, 2436–2448.
(59) Li, W.; Shi, A.-C. *Macromolecules* **2009**, *42*, 811–819.
(60) Xu, Y.; Li, W.; Qiu, F.; Yang, Y.; Shi, A.-C. *J. Phys. Chem. B* **2010**, *114*, 14875–14883.